08,10

Structure and electrochemical characteristics of silver-doped composites based on multi-walled carbon nanotubes and K_xMnO_2 oxide

© S.N. Nesov[1], I.A. Lobov[1], S.A. Matyushenko[1], E.V. Knyazev[1], V.V. Bolotov [1], E.S. Zemskov[1], E.V. Zhizhin[2], A.V. Koroleva [2], E.A. Grigoriev[2]

[1] Omsk Scientific Center, Siberian Branch, Russian Academy of Sciences, Omsk, Russia
[2] St. Petersburg State University, St. Petersburg, Russia

E-mail: nesov55@mail.ru

Received June 2, 2025
Revised June 2, 2025
Accepted June 17, 2025

The mechanisms of composites formation based on multi-walled carbon nanotubes (MWCNTs) and silver-doped K_xMnO_2 oxide obtained by treating MWCNTs in an aqueous solution of $KMnO_4$ with the addition of $AgNO_3$ were studied. The crystal structure and chemical state of the composites obtained with different synthesis times were analyzed. It was shown that with a short synthesis time, defective MnO_{2-x} oxide is predominantly formed on the MWCNT surface, which, in the case of doping, additionally contains double oxides Ag_xMnO_2. With an increase in the synthesis time, composites are formed containing predominantly layered K_xMnO_2 oxide, which, in the case of doping, contains Ag_xMnO_2 oxides and $Ag_{2-x}O$ oxide nanoparticles. Analysis of electrochemical characteristics showed that doping of the composite provides a noticeable increase in specific capacitance up to ~ 201 F/g at a discharge current density of 0.1 A/g versus 148 F/g for the undoped composite.

Keywords: supercapacitors, electrode materials, layered manganese oxide, redox reactions.

DOI: 10.61011/PSS.2025.06.61695.154-25

1. Introduction

Layered oxide K_xMnO_2 thanks to wide interplanar spacings (up to 0.7 nm) is a promising material for use as electrode material in hybrid supercapacitors, as well as sodium- and potassium-ion batteries [1–3]. Wide interatomic channels K_xMnO_2 promote easy and reversible intercalation of alkali metal ions (Na, K, Li) from electrolyte, which provides for high and stable electrical capacitance. However, insufficient electroconductivity of oxide K_xMnO_2 [4,5] substantially limits its discharge characteristics.

The solution to the problem of low electroconductivity is the development of composites on the basis of K_xMnO_2 and carbon materials with high values of conductivity and specific surface area (carbon black, activated carbon, graphene, carbon nanotubes etc.) [3,5,6]. Formation of composites using nanostructured carbon materials makes it possible to produce a nanocrystalline oxide K_xMnO_2, which may have higher electrochemical characteristics due the increased surface area of the active surface.

The electroconductivty of oxide K_xMnO_2 may also be increased by doping with metals and electroconductive metal oxides [7,8]. Besides, doping may optimize other characteristics of materials, for example, their morphology, cyclic stability, electrochemical activity, and also impact the adhesion of oxide K_xMnO_2 to the surface of the carbon component [9–11].

To deposit the nanoparticles of either the layers of metals/metal oxides on the surface of the nanostructured carbon, often liquid chemical methods are used [12], since they are affordable and may be scaled to the volumes of serial production. However, formation of composite materials (especially nanostructured ones) — is a complicated process that requires monitoring of parameters for reproducible production of materials with stable characteristics.

This paper studied the structure and electrochemical characteristics of silver-doped composites based on multi-walled carbon nanotubes (MWCNTs) and oxide K_xMnO_2. These composites were formed by liquid deposition of oxides on the surface of MWCNTs from aqueous solution of $KMnO_4$ with addition of $AgNO_3$. One of the main objectives of the paper was to determine the kinetics of composite structure and chemical composition formation depending on the synthesis time. The most desired structure of the composite is MWCNTs coated with a solid layer of oxide K_xMnO_2, having the thickness of nanoscale size (units or dozens of nanometers). Besides, electrochemical activity of the composite will be determined by the state of the surface layer of oxide K_xMnO_2, the chemical composition of which may be studied using surface-sensitive methods of analysis, such as, for example, X-ray photoelectron spectroscopy (XPS). It is known that the structure and chemical state of oxide near the interface „MWCNTs surface-metal oxide“ to a significant degree determines the charge transport processes. Therefore, the paper studies the composites produced within a short synthesis time in order to identify the features of the chemical state in a metal

Table 1. Conditions for synthesis of composites and their notational conventions

Notational convention of composite	Time of synthesis, h	MWCNTs, g	$KMnO_4$, g	$AgNO_3$, g
C_Mn_1	0.5	0.30	3.0	–
C_Mn_2	6.0			–
C_MnAg_1	0.5			0.15
C_MnAg_2	6.0			0.15

oxide component near the interface layer. It is evident that the mechanism for composite structure formation must vary with the increase of the synthesis time, since initially the solution interacts directly with the MWCNTs surface. As the quantity of manganese oxide increases on the MWCNTs surface, the solution will interact now mostly with a layer of the formed oxide. The study of these aspects will help to make the selection of the models for formation of electrode materials to achieve a complex of the necessary electrochemical characteristics.

2. Experiment

2.1. Forming the composites

The paper used MWCNTs with diameter $\sim 7-10$ nm (MWCNTs-1, Institute of Catalysis, Siberian Branch of the Russian Academy of Sciences, Novosibirsk) [13]. To improve the hydrophility, MWCNTs were treated in 30% HNO_3 for 0.5 h with subsequent washing in distilled water. In order to separate the bundles and agglomerates of MWCNTs, they were treated with ultrasound in distilled water for 1 h. Then aqueous suspension of MWCNTs was heated to 60°C being permanently mixed with the speed of $25\,s^{-1}$ in a magnetic mixer. Prior to the start of synthesis, aqueous solutions $KMnO_4$ and $AgNO_3$ were prepared separately, which were also heated to 60°C and added to MWCNTs suspension. Temperature of the reaction solution (60°C) and rate of its mixing ($25\,s^{-1}$) were constant for the entire duration of synthesis. Qualitative ratios of precursors, time of synthesis and notational conventions of composites are given in Table 1. The produced composites were many times washed with distilled water and dried at 1 Pa and 80°C for 6 h.

2.2. Analysis of structure and chemical condition of composites

The crystalline structure of composites was analyzed by the method of transmission electron microscopy (TEM) using electron microscopes JEM-2100 („JEOL", Japan) (equipment of the Omsk Regional Center of Collective Use, Siberian Branch, Russian Academy of Sciences), and Zeiss Libra 200 FE („Carl Zeiss", Germany) (equipment of Interdisciplinary Resource Center „Nanotechnologies" of St. Petersburg State University). Microphotographs were taken in a bright-field mode with the accelerating voltage of 200 kV. The values of the maximum resolution in the lines for these microscopes are $0.14-0.12$ nm.

The chemical state of the specimens were analyzed by XPS method in the Resource Center „Physical Methods of Surface Studies" of St. Petersburg State University using a photoelectron spectrometer „Escalab 250Xi" with radiation of Al-Kα (photon energy 1486.6 eV). XPS spectra were recorded in the mode of constant transmission energy at 100 eV for survey spectra (energy step size 1.0 eV) and 50 eV for spectra of core levels of elements (energy step size 0.1 eV) at room temperature and under ultrahigh vacuum ($\sim 1 \cdot 10^{-7}$ Pa) in the analysis chamber. The combined ion-electronic charge compensation system was used to remove the sample charge. The diameter of the X-ray spot on the specimen surface was $\sim 650\,\mu$m, the thickness of the analyzed layer was $\sim 3-5$ nm.

2.3. Analysis of electrochemical characteristics

Electrodes for electrochemical measurements were produced by mixing the synthesized composite and polyvinylidenfluoride in the proportion of 9 : 1 by mass in 1-methyl-2-pyrrolidone. The produced viscous mass was rolled to form thin sheets used to cut wafers with size of $10 \times 5 \times 0.3$ mm.

The electrochemical studies were carried out in a three-electrode cell with a platinum counter electrode and a Ag/AgCl reference electrode. As electrolyte, a 1M solution of Na_2SO_4 was used. All measurements were carried out on air at temperature equal to 20°C. To assess the redox reactions, the electrodes were studied by the method of cyclic voltammetry (CV) in the potential window from 0 to 0.8 V relative to Ag/AgCl. The value of the specific capacitance of electrodes was calculated from the dependences of the galvanostatic charge/discharge by method of energy conversion in a discharge area [14] at current densities from 0.1 to 2.0 A/g. Besides, after the maximum potential 0.8 V was reached, in process of charging the electrode was additionally charged for 5 min in a potentiostatic mode (charge mode „direct current/direct voltage"). To calculate the specific capacitance, only the mass of active material (composite) was taken into account in the electrode (90% of the total mass of electrode).

3. Results and discussion

TEM images of composite C_Mn_1 show nanoparticles on the surface of MWCNTs, which have an ordered crystalline structure, where, according to the fast Fourier transform (FFT) data, the value of Interlayer distance is $0.23-0.28$ nm (Figure 1, *a*). This complies with one of the values of interplanar spacings specific for oxide β-MnO_2 [15]. The values of Interlayer distance in the MWCNTs walls are $0.34-0.35$ nm.

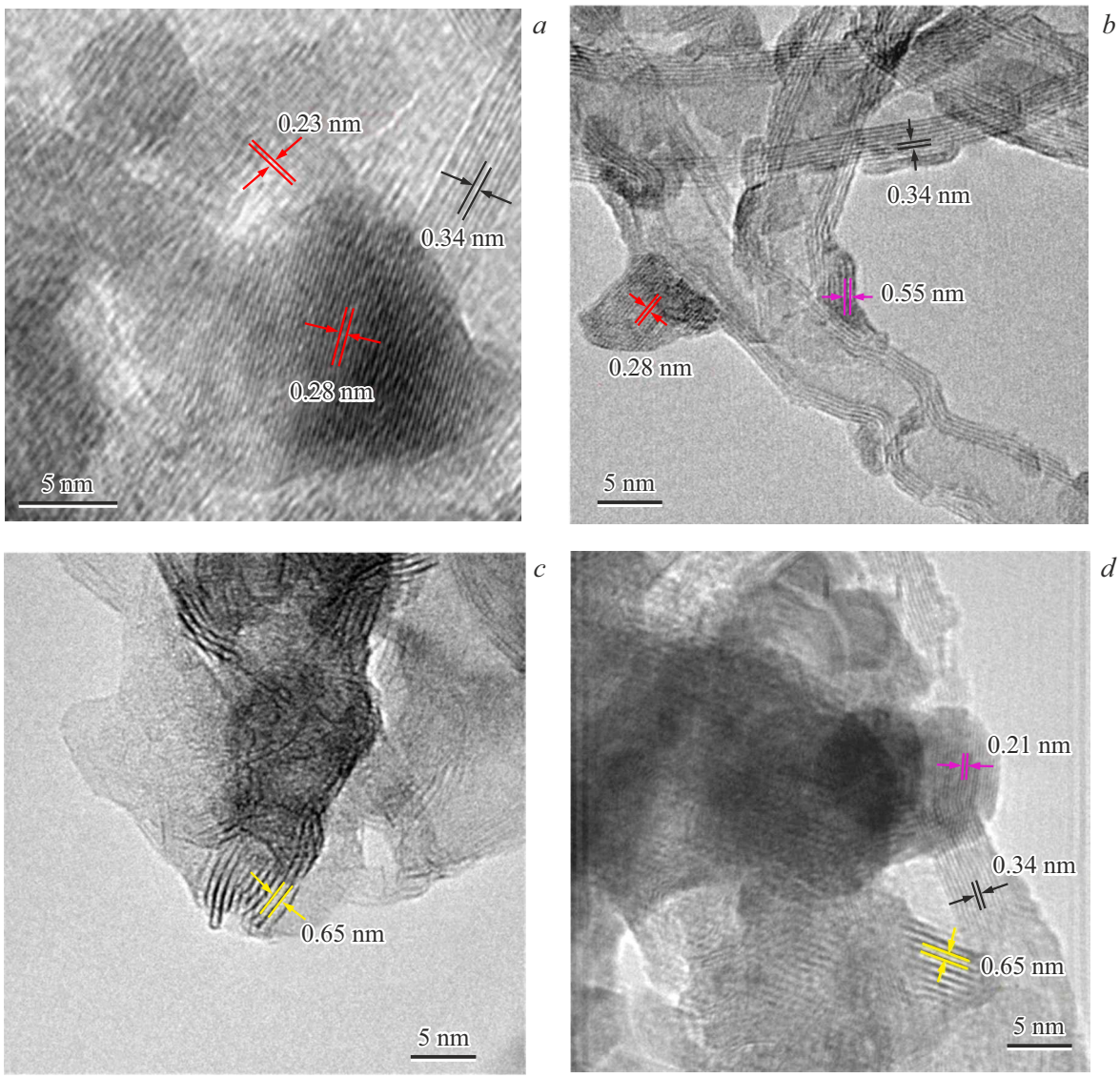

Figure 1. TEM images of composites: *a* — C_Mn_1; *b* — C_MnAg_1; *c* — C_Mn_2; *d* — C_MnAg_2.

TEM images of composite C_MnAg_1 shows a noticeably high number of metal oxide particles on the MWCNTs surface in the form of amorphous and crystalline inclusions (Figure 1, *b*). The analysis by FFT method showed the presence of particles with Interlayer distance specific for MnO_2 (0.23−0.28 nm) and Ag_xMnO_2 (0.55 nm) [16].

TEM images of composite C_Mn_2 on the MWCNTs surface show the chaotically oriented nanocrystallites of manganese oxide (Figure 1, *c*). The main part of crystallites in one of the directions has the dimensions of the order of nm units and consists of several atomic layers. In certain areas these crystallites fully cover the surface of MWCNTs, forming a layer with thickness of up to $\sim$ 15 nm. The analysis of the values of interplanar spacings by FFT method shows that they are in the range of 0.63−0.65 nm, which may correspond to oxide δ-MnO_2 or oxide K_xMnO_2 [5,17,18]. Inclusions of amorphous manganese oxide in this composite are quite rare, and are practically absent in most TEM images.

TEM images of composite C_MnAg_2 (Figure 1, *d*) also show chaotically oriented nanocrystallites on the MWCNTs surface — K_xMnO_2 (values $d \sim 0.63-0.65$ nm), however, the content of amorphous inclusions is much higher compared to composite C_Mn_2. Besides, the composite also includes denser evenly distributed nanoparticles of sphere-like shape, the diameter of which is $\sim$ 1−15 nm. According to the FFT data, the particles have crystalline structure, where the values of Interlayer distance are 0.20−0.22 nm, which may be compliant with either metal Ag, or $Ag_{2-x}O$ oxide (ICDD PCPDFWIN V.2.2 #87-0720, #76-1393).

Figure 2, *a* shows the survey XPS-spectra of the studied composites. The quantitative results of the elemental analysis performed using the panoramic spectra by method of elemental sensitivity coefficients are listed in Table 2. The

Table 2. Results of quantitative elemental analysis of composites according to XPS data

	Concentration, at.%								Δ Mn3*s*, eV	μ(Mn)
	C	O	Mn	K	Ag	O/Mn	K/Mn	Ag/Mn		
C_Mn_1	86.9	9.8	3.4	0.05	–	2.88	0.01	–	4.58	3.85
C_MnAg_1	82.7	11.6	4.9	0.05	0.8	2.37	0.01	0.16	4.78	3.60
C_Mn_2	38.8	37.3	19.8	4.1	–	1.88	0.21	–	4.75	3.64
C_MnAg_2	45.0	33.4	17.8	2.8	1.1	1.87	0.16	0.06	4.93	3.41

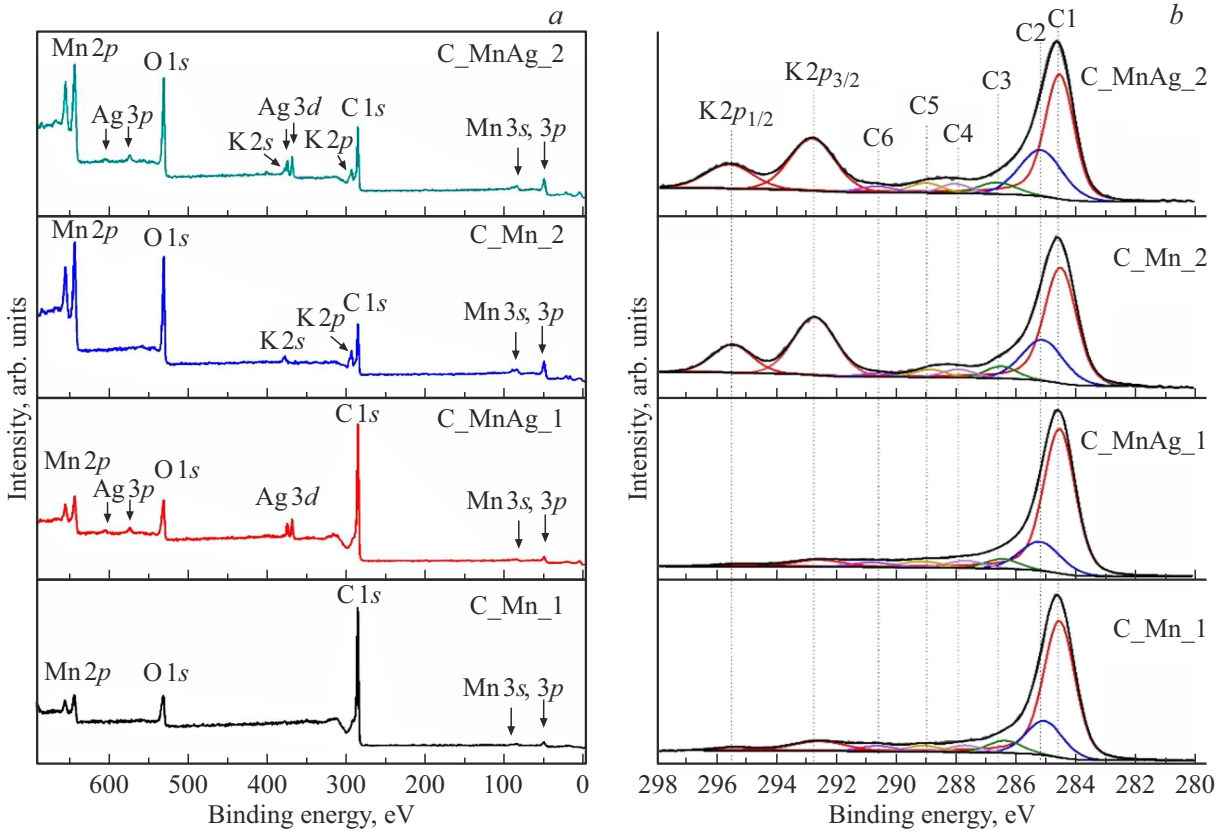

Figure 2. XPS spectra of initial and doped composites obtained at various synthesis time: *a* — survey spectra; *b* — C1s; *c* — Mn3s; *d* — O1s; *e* — Ag3*d*.

remarkable thing is the fact that there are rather intense lines of potassium (K2*s*, 2*p*) in XPS spectra of the source and doped composites produced from a longer time of formation (C_Mn_2 and C_MnAg_2), and very low intensity of lines K2*s* and 2*p* in the survey spectra of composites formed for a shorter time (C_Mn_1 and C_MnAg_1) (Figure 2, *a*). The presence of some potassium in the latter is validly confirmed only by analysis of the spectra of core lines C1*s* (Figure 2, *b*), and for composite C_MnAg_1 — spectrum of line Ag3*d* (Figure 2, *e*), the energy ranges of which partially overlap with the lines of potassium K2*p* and 2*s*.

Comparing the results of quantitative XPS analysis for composites formed within a shorter time of synthesis (C_Mn_1 and C_MnAg_1), you may note a much higher concentration of manganese (approximately by 50% higher) in the doped composite (Table 2). This result agrees well with the results of the TEM analysis of these composites. For both specified composites there is a rather high ratio of O/Mn concentrations indicating oxidation of MWCNTs surface. Besides, the MWCNTs surface in the doped composite is oxidized not so significantly (Table 2).

O/Mn values for composites obtained from a longer time of synthesis (C_Mn_2 and C_MnAg_2) are close and make ~ 1.9. TEM data, and the presence of potassium in these composites, indicate the formation of double oxide K_xMnO_2.

Comparison of the results of quantitative analysis for the doped composites formed during different times of synthesis (C_MnAg_1 and C_MnAg_2) shows that the relative content of silver decreases as the time of composite formation

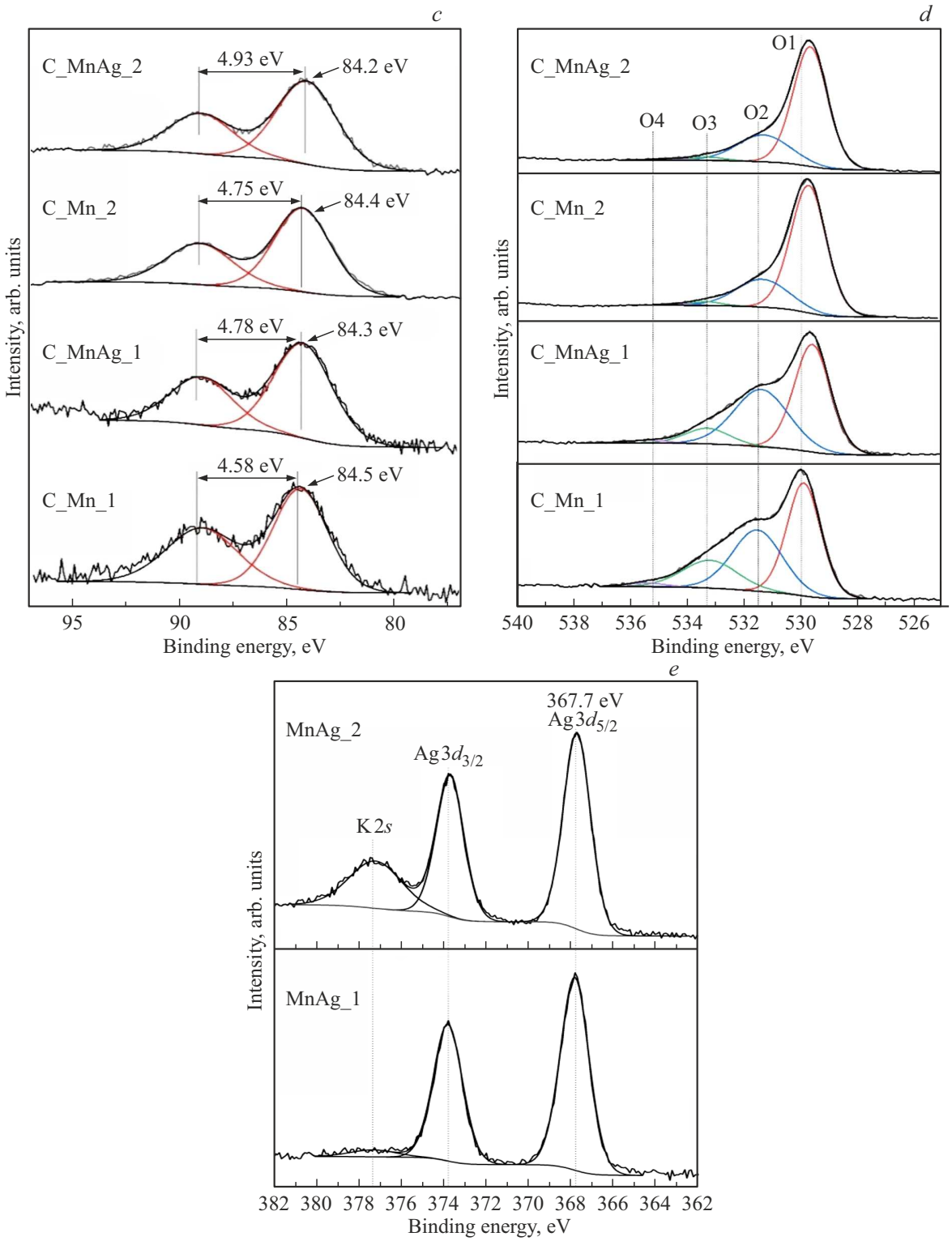

Figure 2 (*Contd*).

increases — ratio of Ag/Mn concentrations for the specified composites differs more than 2 times (Table 2). It may be assumed that in composite C_MnAg_2 the maximum degree of doping with silver is observed near the interface „MWCNTs surface-metal oxide".

Note that the low concentration of potassium in composites C_Mn_1 and C_MnAg_1 (Table 2) agrees well with the TEM data, which showed the presence of only MnO_2 crystallites in the first of the specified composites. For the doped composite (C_MnAg_1) the presence of crystallites

with Interlayer distance ~ 0.55 nm (Figure 1, *b*) may support the potential formation of compounds Ag_xMnO_2.

The energy range of a photoelectron line C1*s* overlaps with the range of K2*p* (Figure 2, *b*). XPS C1*s* spectra of composites were approximated by a set of 6 components that were compliant with carbon in different chemical states: C1 — sp^2-carbon (MWCNTs frame); C2 — defects in MWCNTs walls,bond and also carbon atoms located near the oxygen groups fixed on the MWCNTs surface; C3, C4, C5 — carbon within C−O, C=O, COOH, accordingly; component C6 — carbon within carbonate complexes [19–21]. In the high-energy area of the spectrum (binding energy 293−296 eV) of the composites produced within a longer time of synthesis (C_Mn_2 and C_MnAg_2), intense lines of doublet K2*p* are observed, whereas in the spectra of composites produced within a shorter time of synthesis, the intensity of the potassium lines hardly exceeds the background level. The analysis of the composite spectra shows that the increase in time of formation of composites causes the increase in the quantity of oxygen-containing groups on the MWCNTs surface, besides, the maximum relative increase in intensity is observed for the components compliant with carbon within C=O- and COOH-groups (Figure 2, *b*). Previously it was shown [22] that metal oxides were sorbed on the surface of MWCNTs, as a rule, with the participation of the functional groups with a double C=O bond.

To analyze the chemical condition of manganese, XPS spectra Mn3*s* were used (Figure 2, *c*). It is known [5,23–25] that the energy distance between the maxima of doublet Mn3*s* is determined by the charge state of manganese. In paper [25] they propose an empirical formula to determine the charge state of manganese (μ) using an energy gap ΔMn3*s*:

$$\mu(\mathrm{Mn}) = 9.67 - 1.27 \cdot \Delta\mathrm{Mn3}s. \quad (1)$$

Value $\mu = 3.85$ for composite C_Mn_1 (Table 2) in a combination with the results of the quantitative analysis, which showed low content of potassium in composite, makes it possible to speak about the presence of Mn(IV) oxide with a small deficit of oxygen (MnO_{2-x}). Composite C_MnAg_1 also practically does not contain potassium, however, the value $\mu = 3.60$ in this case is much lower (Table 2). It may be assumed that the decrease in the charge state of manganese is provided for by the formation of double oxide compounds (Ag_xMnO_2), where a silver ion may partially screen a negative oxygen charge. Low value $\mu = 3.64$ for composite C_Mn_2 in a combination with high concentration of potassium indicates the presence of oxide K_xMnO_2. This fully agrees with the TEM data. An even lower value $\mu = 3.41$ for composite C_MnAg_2 may be provided for by a combination of factors: formation of oxide K_xMnO_2, and impact of the present silver (formation of compounds Ag_xMnO_2).

XPS O1*s* spectra were approximated using a set of 4-components (Figure 2, *d*), compliant with oxygen: in a chemical bond with metals (O1), within double C=O and single C−O bonds (O2 and O3, accordingly), and also oxygen within adsorbed water (O4) [5,21,26]. A noticeable shift is observed in the position of maximum O1 in the spectra of composites C_MnAg_1, C_Mn_2 and C_MnAg_2, which contain silver and/or potassium, relative to the spectrum of composite C_Mn_1, where manganese oxide practically does not contain impurity atoms. The most noticeable is the fact of negative shift of maximum in the O1 component in the spectrum of composite C_MnAg_1, containing silver and practically not containing potassium. This indicates the potential formation of Ag_xMnO_2 oxides. From the analysis of the oxygen spectra, it also follows that oxidation of MWCNTs in formation of composites happens mostly due to the formation of C=O-bonds (component O2), which agrees with the analysis of C1*s* spectra. Besides, stronger oxidation is confirmed for the MWCNTs surface for composite C_Mn_1 compared to composite C_MnAg_1 — relative integral intensity of component O1 for these composites is 44 and 50% accordingly.

The position of the main maximum in XPS spectra Ag3*d* coincides for composites C_MnAg_1 and C_MnAg_2 (Figure 2, *e*) and is 367.8 eV, which, according to [27], may be compliant with oxide Ag_2O.

The produced results on the structure and the chemical state of the studied components show that as the synthesis time increases, seemingly the mechanism of potassium permanganate decomposition mechanism changes. It is established that at the small synthesis time (regardless of the presence of $AgNO_3$) manganese oxide is formed on the surface of MWCNTs, which practically contains no potassium in its composition. Additionally the results of XPS and TEM indicate that when the composite is doped with silver, it is possible that Ag_xMnO_2 oxides will be formed. It is found that doping causes increased concentration of manganese, and also promotes lower oxidation of the surface of carbon nanotubes.

In a undoped composite obtained within a long time of synthesis (C_Mn_2), manganese is present mostly as a crystalline oxide K_xMnO_2. In a composite doped with Ag (C_MnAg_2), silver is present both in the form of nanoparticles of defective oxide Ag(I), and in the form of oxides Ag_xMnO_2. Seemingly, the last fact causes a decrease in the extent of crystallinity of a metal oxide component, which you can see in TEM images.

The produced results make it possible to assume the following mechanisms of composite formation. Initially the process of potassium permanganate decomposition may happen with the participation of carbon atoms on the MWCNTs surface by reactions (2)−(3), or also without participation of carbon by reaction (4):

$$4KMnO_4 + 4C + O_2 \rightarrow 4MnO_2 + 2K_2CO_3 + 2CO_2, \quad (2)$$

$$4KMnO_4 + 3C + H_2O \rightarrow 4MnO_2 + K_2CO_3 + 2KHCO_3, \quad (3)$$

$$4KMnO_4 + 2H_2O \rightarrow 4MnO_2 + 3O_2 + 4KOH. \quad (4)$$

In all reactions (2)–(4) potassium forms soluble compounds and transfers to a solution. Probably, as a result of this the composites produced within short time of synthesis have manganese oxide practically undoped with potassium on the MWCNTs surface. Also note that reactions (2)–(3) must result in a formation of defects in a graphene structure of outer layers of MWCNTs with subsequent oxidation, which was found using data of XPS.

If a doped Ag composite is formed, the ion exchange reaction may also occur with formation of silver manganate:

$$AgNO_3 + KMnO_4 \rightarrow AgMnO_4 \downarrow + KNO_3. \quad (5)$$

Then the formed silver manganate is seemingly reduced to compounds Ag_xMnO_2, since according to XPS data manganese in the composite has a charge state between 3^+ and 4^+. Besides, formation of Ag_xMnO_2 may happen due to the reaction between the formed manganese oxide (by reactions (2)–(4)) and silver ions:

$$(MnO_2)^- + Ag^+ \rightarrow AgMnO_2. \quad (6)$$

Formation of poorly soluble compounds Ag_xMnO_2 may provide for the increase of manganese concentration, and the total quantity of metal oxide particles on the MWCNTs surface in composite C_MnAg_1 compared to composite C_Mn_1 (Figure 1, *a* and *b*, Table 2). These particles close the MWCNTs surface from interaction with the oxidizing medium of the reaction solution (first of all, with ions $(MnO_4)^-$), which, according to XPS data, provides for less considerable oxidation of MWCNTs surface in the doped composite.

Formation of lamellar oxide K_xMnO_2, based on TEM and XPS date, is observed only for composites with the increased synthesis time. Accordingly, you may assume that the process of formation K_xMnO_2 „is activated" upon achievement of certain conditions. We believe that formation of K_xMnO_2 happens in accordance with the following scheme. As the quantity of manganese oxide increases on the MWCNTs surface, potassium permanganate decomposes mostly without involvement of carbon (by reaction (4)). This causes increase in the pH level of the solution at the expense of the increase in the concentration of ions $(OH)^-$. Under these conditions the hydrated MnO_2 oxide is partially reduced:

$$MnO_2 \cdot H_2O + e^- \rightarrow MnOOH + OH^-. \quad (7)$$

The formed manganese metahydroxide at high concentration of ions $(OH)^-$ interacts with ions of potassium and silver present in the solution to form complex oxides:

$$MnOOH + K^+ + OH^- \rightarrow K_xMnO_2 + H_2O, \quad (8)$$

$$MnOOH + Ag^+ + OH^- \rightarrow Ag_xMnO_2 + H_2O. \quad (9)$$

Increase of ion $(OH)^-$ concentration in the reaction solution for the case of the doped composite also supports silver deposition in the form of the oxide:

$$Ag^+ + OH^- \rightarrow [AgOH] \rightarrow 1/2Ag_2O + 1/2H_2O. \quad (10)$$

This seemingly explains the presence of silver nanoparticles in the doped composite produced within the longer synthesis time.

The redox reactions happening on the surface of the manganese oxide in aqueous solution of Na_2SO_4 in process of charge / discharge on the positive electrode of the electrochemical cell may schematically be presented as follows [5,28]:

$$MnOOMx + nSO_4^{2-} \leftrightarrow MnO_2//(SO_4)_n^{2-} + xM^+ + xe^-, \quad (11)$$

where M^+ — ions of Na^+ or H^+, specifically adsorbed on the surface from electrolyte, or ions K^+ or Ag^+, present within the composition of complex oxides K_xMnO_2 and Ag_xMnO_2, and sign // — electric double layer.

The analysis of redox reactions happening in the process of charge / discharge on the electrodes obtained from composites was carried out by the CV method at low potential scan rates (Figure 3, *a*). You can see that no pronounced redox maxima are observed on the voltamperogram of composite C_Mn_1. Based on the data on the structure and composition of composites, you can ay that the charge accumulation in this case is implemented mainly with the participation of the Na^+ ions specifically sorbed on the surface of particles MnO_{2-x}. The voltamperogram of the electrode based on composite C_MnAg_1 has a pronounced extended peak (0.22–0.38 V) of a complex shape on the oxidation branch (at the positive potential sweep), which is caused by the redox reactions (11) with participation of oxide Ag_xMnO_2 and subsequent adsorption of ions from electrolyte (Na^+, H^+) upon reduction.

The voltamperogram of the electrode based on C_Mn_2 has paired redox peaks of around 0.38 and 0.15 V on the cathode and anode branches, accordingly, which may be compliant with oxidation of K_xMnO_2 upon potassium removal with subsequent reduction with participation of electrolyte ions (Na^+, H^+, K^+). Comparison of the form of oxidation peaks on voltamperograms of electrodes C_MnAg_1, C_Mn_2 and C_MnAg_2 makes it possible to assume that in the last case the reaction (11) happens with participation of K_xMnO_2 and Ag_xMnO_2 oxides. At the same time, a noticeable shift of oxidation maximum towards the lower potential values is observed on the voltamperogram of electrode C_MnAg_2, which indicates the increase in the redox reactions rate.

Comparison of the curves of galvanostatic discharge for composites C_Mn_1 and C_MnAg_1 (Figure 3, *b*) shows that the latter is characterized by the shorter time of discharge (and, accordingly, the lower specific capacitance). Taking into account of the results of TEM and XPS, which showed the higher content of metal oxide particles on the surface of MWCNTs in composite C_MnAg_1 (compared to composite C_Mn_1), you can assume that the electrochemical activity of compounds Ag_xMnO_2 in the absence of potassium is relative low compared to the activity of MnO_2 oxide. Maximum value of the specific capacitance of composites C_Mn_1 and C_MnAg_1 (at discharge current density

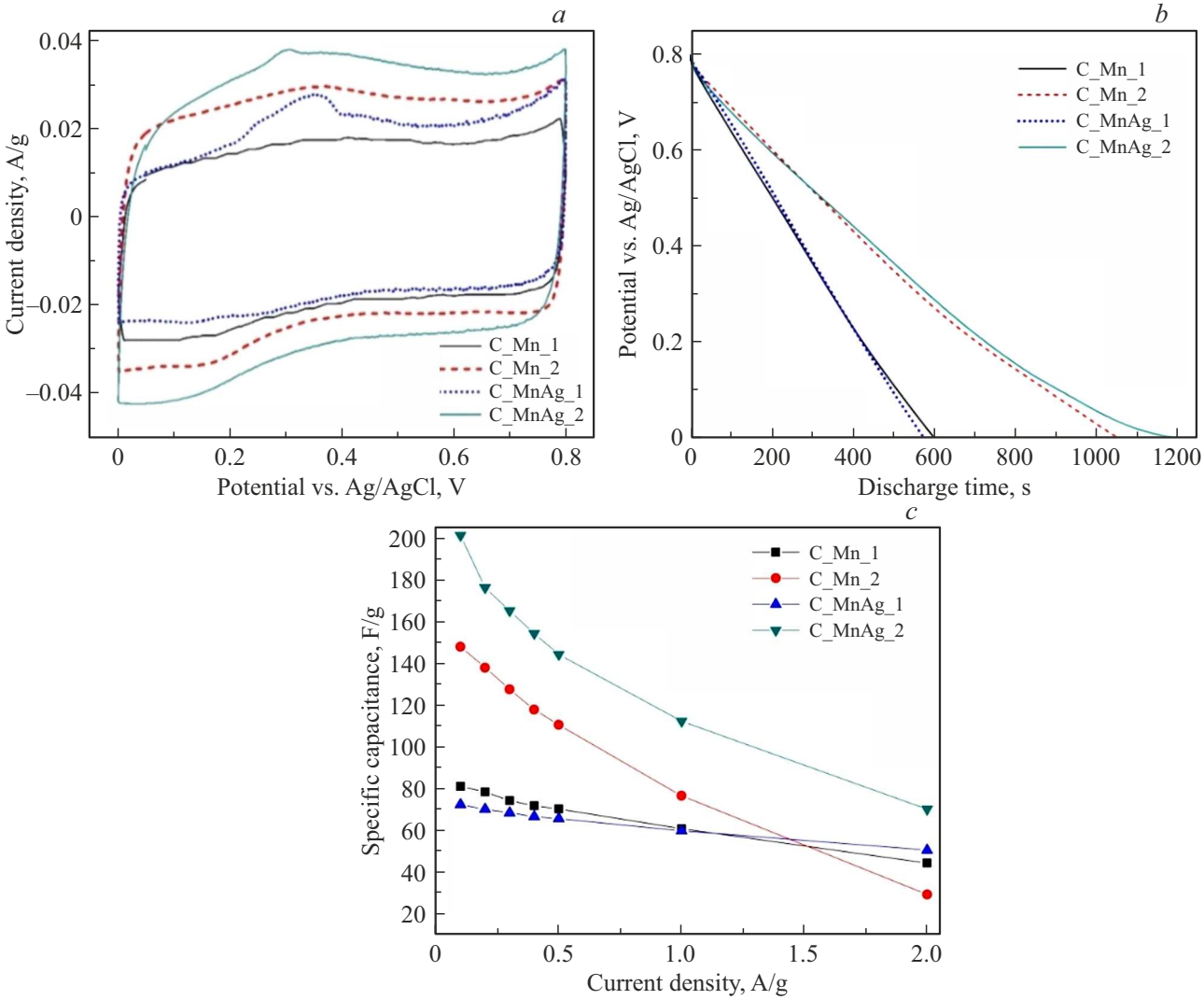

Figure 3. Results of electrochemical measurements: *a* — cyclic voltamperograms of electrodes obtained at the scan rate 0.2 mV/s; *b* — galvanostatic discharge curves at current density of 0.1 A/g; *c* — dependence of the specific capacitance of composites on the discharge current density.

of 0.1 A/g) is ~ 81 and ~ 72 F/g accordingly (Figure 3, *c*). This confirms low electrochemical activity of the doped composite. When the current density increases to 2.0 A/g, the capacitance of composites decreases accordingly to ~ 44 and ~ 50.2 F/g, which in relative terms is 54 and 70% of the maximum value. Increase of the rate capability is usually related to increase in the electroconductivity of the material, however, the measurements of the specific conductivity of electrodes with a four-probe method showed that the values for electrodes C_Mn_1 and C_MnAg_1 are practically the same (~ 110 S/m), which is probably related to low content of metal oxides in these composites.

The analysis of the galvanostatic discharge curves of composites C_Mn_2 and C_MnAg_2 (Figure 3, *b*) shows that in the low potential field the discharge curves have significant deviations from the linear dependence, which indicates high contribution of redox reactions to the charge accumulation. Besides, this deviation for the electrode based on C_MnAg_2 is more significant, which in a combination with a longer discharge indicates higher electrochemical activity of this composite in electrolyte. The obtained data makes it possible to say that the presence of silver in the composite (in the form of Ag_2O nanoparticles, as well as complex oxide compounds), provides for higher electrochemical activity of K_xMnO_2 oxide, which, most probably, is achieved due to the lowering of redox reactions potential (11). This, in its turn, may provide for faster and deeper diffusion of potassium ions into the interatomic channels of layered K_xMnO_2 oxide. The values of the maximum specific capacity (at discharge current density 0.1 A/g) of electrodes based on C_Mn_2 and C_MnAg_2 are ~ 148 and ~ 201 F/g accordingly (Figure 3, *c*). As the current density increases to 2.0 A/g, the specific capacitance decreases to ~ 30 and ~ 70 F/g accordingly (19.7 and 34.5% of the maximum

capacitance). Higher rate capability of the doped composite in this case is also provided for by higher electroconductivity. The measured values of specific conductivity of electrodes based on C_Mn_2 and C_MnAg_2 are ~ 8 and ~ 14 S/m.

4. Conclusion

The paper studied the structure, the chemical state and electrochemical characteristics of the composites produced by soaking MWCNTs in the aqueous solution of $KMnO_4$ with addition of $AgNO_3$ for doping of the material with the electroconductive component. The objects of comparison in the paper were composites synthesized without addition into solution $AgNO_3$. It was found that the mechanism of metal oxide component formation on the surface of carbon nanotubes changes substantially as the time of synthesis increases. TEM and XPS methods found that regardless of the presence of $AgNO_3$ in the solution at short time of synthesis (30 min), MnO_{2-x} is formed on the MWCNTs surface, which practically does not contain potassium in its composition. As the time of synthesis increases, MWCNTs are coated with nanocrystals of K_xMnO_2 oxide, which in case of doping also contain nanoparticles of crystalline $Ag_{2-x}O$ oxide. It was shown that Ag doping causes increased adsorption of manganese oxide on the surface of MWCNTs, possibly due to the formation of poorly soluble compounds Ag_xMnO_2, which form a dense layer preventing oxidation of carbon nanotubes in process of interaction with the oxidizing medium of the reaction solution.

The analysis of the electrochemical characteristics of electrodes showed that the composites produced within the long synthesis time (6 h) have the highest specific capacitance. And Ag doping provides for noticeable growth of the maximum specific capacitance (at least 35% vs. the undoped composite), probably due to the increase in the electrochemical activity of K_xMnO_2 oxide. The values of the specific discharge capacitance of the doped composite in 1M Na_2SO_4 electrolyte are ~ 201 and ~ 70 F/g at the current density values of 0.1 and 2.0 A/g, accordingly.

The results obtained in the paper may be used to select the modes for formation of nano-composites based on carbon materials and manganese oxide for chemical current sources and other applications.

Acknowledgments

The studies by XPS and TEM method were carried out on a non-finance basis using the equipment of Resource Centers „Physical Methods of Surface Research“ and „Nanotechnologies“ of the St. Petersburg State University (projects 125021902439-8 and AAAA-A19–119091190094). The paper also used the transmission electron microscope of the Omsk Regional Center of Collective Use, Siberian Branch of the Russian Academy of Sciences.

Funding

The study was performed under framework of State Assignment of Omsk Scientific center of Siberian Branch of Russian Academy of Science (state registration number of project 121021600004-7).

Conflict of interest

The authors declare that they have no conflict of interest.

References

[1] N. Liu, X. Zhao, B. Qin, D. Zhao, H. Dong, M. Qiu, L. Wang. J. Mater. Chem. A **10**, 25168 (2022). DOI: 10.1039/D2TA06681E
[2] Z. Zhao, Y. Sun, Y. Pan, J. Liu, J. Zhou, M. Ma, X. Wu, X. Shen, J. Zhou, P. Zhou. J. Colloid Interface Sci. **652**, 231 (2023). DOI: 10.1016/j.jcis.2023.08.055
[3] L. Chen, Y. Zhang, C. Hao, X. Zheng, Q. Sun, Y. Wei, B. Li, L. Ci, J. Wei. ChemElectroChem **9**, e202200059 (2022). DOI: 10.1002/celc.202200059
[4] G. He, Y. Duan, L. Song, X. Zhang. J. Appl. Phys. **123**, 214101 (2018). DOI: 10.1063/1.5021614
[5] S.N. Nesov, I.A. Lobov, S.A. Matyushenko, E.A. Grigoriev. ECS J. Solid State Sci. Technol. **13**, 101002 (2024). DOI: 10.1149/2162-8777/ad8517
[6] Z. Pan, C. Yang, Y. Li, X. Hu, X. Ji. Chem. Eng. J. **428**, 131138 (2022). DOI: 10.1016/j.cej.2021.131138
[7] S.N. Nesov, I.A. Lobov, S.A. Matyushenko, V.V. Bolotov, K.E. Ivlev, D.V. Sokolov, Yu.A. Stenkin. FTT **65**, 2033 (2023). (in Russian). DOI: 10.61011/FTT.2023.11.56563.196
[8] R. Ai, X. Zhang, S. Li, Z. Wei, G. Chen, F. Du. Chem. Eur. J. **30**, e202400791 (2024). DOI: 10.1002/chem.202400791
[9] I. Oda-Bayliss, S. Yagi, M. Kamiko, K. Shimada, H. Kobayashi, T. Ichitsubo. J. Mater. Chem. A **12**, 17510 (2024). DOI: 10.1039/D4TA00659C
[10] A. Ochirkhuyag, T. Varga, I. Y. Tóth, Á.T. Varga, A. Sápi, Á. Kukovecz, Z. Kónya. Int. J. Hydrog. Energy **45**, 16266 (2020). DOI: 10.1016/j.ijhydene.2020.04.022
[11] D.R. Jones, H.E.M. Hussein, E.A. Worsley, S. Kiani, K. Kamlungsua, T.M. Fone, C.O. Phillips, D. Deganello. ChemElectroChem. **10**, e202300210 (2023). DOI: 10.1002/celc.202300210
[12] P. Pazhamalai, V. Krishnan, M.S. Saleem, S. Kim, H. Seo. Nano Convergence **11**, 30 (2024). DOI: 10.1186/s40580-024-00437-2
[13] V.L. Kuznetsov, D.V. Krasnikov, A.N. Schmakov, K.V. Elumeeva. Phys. Stat. Sol. B **249**, 2390 (2012). DOI: 10.1002/pssb.201200120
[14] S.A. Matyushenko, S.N. Nesov. Dinamika sistem, mekhanizmov i mashin **12**, 78 (2024). (in Russian). DOI: 10.25206/2310-9793-2024-12-3-78-86
[15] D. Gangwar, C. Rath. Appl. Surf. Sci. **557**, 149693 (2021). DOI: 10.1016/j.apsusc.2021.149693
[16] O. Mahroua, B. Alili, A. Ammari, B. Bellal, D. Bradai, M. Trari. Ceram. Int. **45**, 10511 (2019). DOI: 10.1016/j.ceramint.2019.02.113
[17] C. Guo, Q. Zhou, H. Liu, S. Tian, B. Chen, J. Zhao, J. Li. Electrochimica Acta **324**, 134867 (2019). DOI: 10.1016/j.electacta.2019.134867

[18] A. Li, C. Li, P. Xiong, J. Zhang, D. Geng, Y. Xu. Chem. Sci. **13**, 7575 (2022). DOI: 10.1039/D2SC02442J
[19] V.V. Bolotov, E.V. Knyazev, S.N. Nesov. Pisma v ZhTF **48**, 11 (2022). (in Russian). DOI: 10.21883/PJTF.2022.05.52148.18864
[20] L.G. Bulusheva, S.G. Stolyarova, A.L. Chuvilin, Yu.V. Shubin, I.P. Asanov, A.M. Sorokin, M.S. Mel'gunov, S. Zhang, Y. Dong, X. Chen, H. Song, A.V. Okotrub. Nanotechnology **29**, 134001 (2019). DOI: 10.1088/1361-6528/aaa99f
[21] V.S. Kovivchak, S.N. Nesov, T.V. Panova. FTT **67**, 50 (in Russian) (2025). DOI: 10.61011/FTT.2025.01.59768.293
[22] S.N. Nesov, P.M. Korusenko, V.A. Sachkov, V.V. Bolotov, S.N. Povoroznyuk. J. Phys. Chem. Solids. **169**, 110831 (2022). DOI: 10.1016/j.jpcs.2022.110831
[23] Benedet, A. Gasparotto, G.A. Rizzi, C. Maccato, D. Mariotti, R. McGlynn, D. Barreca. Surf. Sci. Spectra. **30**, 024018 (2023). DOI: 10.1116/6.0002827
[24] X. Cui, F. Hu, W. Wei, W. Chen. Carbon **49**, 1225 (2011). DOI: 10.1016/j.carbon.2010.11.039
[25] M.L. López, I. Álvarez-Serrano, D.A. Giraldo, P. Almodóvar, E. Rodríguez-Aguado, E. Rodríguez-Castellón. Appl. Sci. **12**, 1176 (2022). DOI: 10.3390/app12031176
[26] O.V. Petrova, D.V. Sivkov, S.V. Nekipelov, A.S. Vinogradov, P.M. Korusenko, S.I. Isaenko, R.N. Skandakov, K.A. Bakina, V.N. Sivkov. Appl. Sci. **13**, 128 (2023). DOI: 10.3390/app13010128
[27] https://xpsdatabase.net/silver-spectra-ag-metal
[28] D.G. Gromadsky. J. Chem. Sci. 128, 1011 (2016). DOI: 10.1007/s12039-016-1084-2

Translated by M.Verenikina